Singlet Fission as the Gateway to Triplet Generation in Heavy Atom-Free Organic Molecules

Takao Tsuneda[**,†,‡] and Tetsuya Taketsugu[†,¶]

†*Department of Chemistry, Faculty of Science, Hokkaido University, Sapporo 060-0810, Japan*

‡*Graduate School of System Informatics, Kobe University, Nada-ku, Kobe, Hyogo 657-8501, Japan*

¶*Institute for Chemical Reaction Design and Discovery (WPI-ICReDD), Hokkaido University, Sapporo 001-0021, Japan*

E-mail: takaotsuneda@sci.hokudai.ac.jp

Abstract

Triplet generations in heavy atom-free organic molecules are primarily revealed to proceed through singlet fissions (SFs) by investigating the contributions of SFs and intersystem crossings to the generation rates. The spin-flip long-range corrected time-dependent density functional theory calculations on 11 organic molecules known for triplet generation under photoirradiation are performed. The correlation between the descriptors for SF and the experimental singlet-to-triplet conversion rates strongly supports the predominance of SF progressions in all these molecules, corroborated by experimental observations of their triplet-triplet annihilations. Based on these findings, we propose an updated conditions for SF progression: There is a high-absorption singlet state just above the triplet-triplet excitation of chromophore dimer, or the singlet (triplet-triplet) excitation itself is responsible for photoabsorption. To the best of our knowledge, all organic molecules known for rapid triplet state generation fulfill these conditions.

Graphical TOC Entry

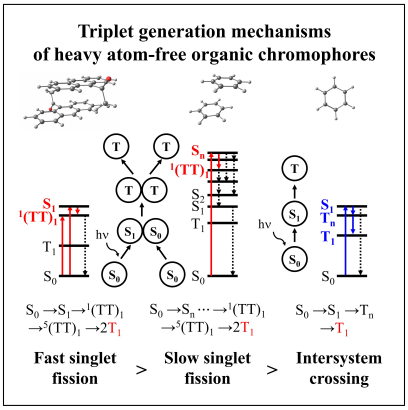

The generation of triplet states in heavy atom-free organic molecules has been explained through intersystem crossing (ISC).[1] ISC involves spin-forbidden transitions between different spin states, driven by relativistic spin-orbit couplings. This process results from the interaction between electron spins and orbital angular momenta, with spin-orbit couplings having the most pronounced effect as a local interaction that usually acts between electrons near heavy atoms. The likelihood of ISC is determined by factors such as the presence of heavy atoms, the energy gap between the lowest singlet excited state (S_1) and the triplet excited state (T_n) just below it, and adherence to the El-Sayed rule,[2,3] which posits that ISC proceeds through transitions between singlet and triplet states involving combinations of $n\pi^*$ and $\pi\pi^*$ states. However, conventional experimental studies have observed that many triplet generation processes in organic molecules significantly deviate from these criteria. Examples include generation processes that are uncorrelated or negatively correlated with heavy atom effects due to spin-orbit couplings,[4,5] processes that proceed rapidly despite a significant S_1-T_n (S-T) energy gap,[6] processes that advance rapidly without adhering to the El-Sayed rule,[7,8] and processes with solvent dependencies unrelated to ISC.[4,9] As findings related to this study, an experimental study shows that the triplet generation rates of benzene deduced from relativistic spin-orbit coupling inducing ISC is so insignificant that it has led to unsupported speculations about conical intersections facilitating ultrafast S-T transitions.[10] A theoretical study on the S-T transitions in nanographene fragments, including pyrene and triphenylene, have also found that the spin-orbit couplings are too small to account for the observed S-T transition rates, even though it assumes that spin-spin interactions, which normally inhibit S-T transitions, play a role in facilitating the triplet generations.[11] These findings suggest the presence of factors other than ISC driving triplet generation reactions in heavy atom-free organic molecules.

Singlet fission (SF) is proposed as an alternative mechanism driving triplet generations in heavy atom-free organic molecules. SF involves the conversion of singlet states (S_n, $n \geq 1$) into triplet-triplet (TT) excited states through a spin-allowed transition. Subsequently, a

spin-forbidden transition occurs from singlet ^{1}(TT) to quintet ^{5}(TT) excited states.[12–14] through the zero-field splitting interaction[15] or the triplet-triplet exchange interaction,[16,17] and the subsequent re-encounter ultimately splitting the quintet ^{5}(TT) state into two T states,[18] if it does not decay to the ground state:

$$\mathrm{S}_0 + \mathrm{S}_n \rightarrow {}^1(\mathrm{TT}) \rightarrow {}^5(\mathrm{TT}) \rightarrow 2\mathrm{T}. \tag{1}$$

SF occurs when the triplet excitation energy is slightly less than half of the singlet excitation energy.[12,19,20]

$$(\mathrm{TT}) \sim 2\Delta E(\mathrm{T}) \lesssim \Delta E(\mathrm{S}_n), \tag{2}$$

where ΔE is the excitation energy. In recent studies, we investigated the possibility of SF in three major heavy atom-free organic photosensitizers: benzophenone, boron-dipyrromethene (BODIPY), and methylene blue. The results confirmed that SF can occur for all these photosensitizers, because these satisfy the conditions for SF progression:[21]

1. Near-degenerate low-lying singlet and (TT) excitations with a significant S_1-T_1 energy gap, and

2. a moderate π-stacking energy of chromophores, higher than but not far from the solvation energy, to facilitate the dissociation and generation of triplet-state chromophores.

Experimental analyses, such as transient absorption spectrum studies, were undertaken to compare and validate the observed results for these photosensitizers. The experimental data robustly support the advancement of SF in these systems. Furthermore, the examination of other heavy atom-free photosensitizers, such as tetramethyl BODIPY derivatives[22] and silicon phthalocyanine used in photoimmunotherapy,[23] revealed solvent dependence in the former and light intensity dependence and reaction acceleration in the latter, indicating SF progression. These findings collectively suggest SF as a plausible common mechanism for

triplet generation in organic molecules.

Various experimental evidence implicitly supports the occurrence of SF in heavy atom-free organic molecules. Notably, TT annihilation, the reverse reaction of SF, leading to delayed fluorescence, has been observed. TT annihilation involves the progression from two triplets (2T) to quintet (^{5}(TT)), then to singlet (^{1}(TT)), and finally to the ground state (S_0) with photon emission.[12] The TT annihilation process suggests the formation of stackings between chromophores in the triplet state, creating an environment conducive to SF. It is acknowledged that the SF rate is influenced by the configuration of the π-stacking arrangement in materials,[24] and that the formation of π-stacking is essential for SF. Furthermore, solvent dependence observed in triplet generation provides another experimental indicator of SF. Since SF involves dimerization, it requires dimerization energy higher than the solvation energy in a solvent, leading to direct solvent dependence. In contrast, ISC proceeds independently, and any changes in the excitation energy are minor, such as the stabilization of charge transfer excitation in polar solvents. Clear solvent dependence has been reported in the triplet generation of many heavy atom-free organic molecules, suggesting the involvement of SF. Moreover, heavy atom effects are often not observed, and the progression can be rapid even when there is a large energy gap between S_1 and the triplet state just below it, violating traditional criteria for ISC. Triplet generation can also occur rapidly, even when S_1 and the triplet states of the de-excitation destination do not satisfy the El-Sayed rule. Therefore, while experimental observations implicitly hint at singlet fission being involved in triplet generation within heavy atom-free organic molecules, explicit experimental evidence directly linking triplet generation in these molecules to singlet fission remains absent.

In this study, we explore the possibility of SF as the driving force behind the rapid generation of triplets in major organic molecules lacking heavy atoms - a phenomenon previously ascribed to ISC, examined from an electronic state perspective. We employ the spin-flip long-range corrected (LC) time-dependent density functional theory (TDDFT),[25] encompassing two-electron excitation correlation and long-range exchange effects. This enables

the treatment of electronic states featuring mixed intra- and intermolecular charge transfer excitations, as investigated in this study. Our primary objective is to assess whether SF can consistently explain previously unexplained experimental results concerning the triplet generation in heavy atom-free organic molecules using this approach.

Excited state calculations were conducted on eleven heavy atom-free organic molecules known for their rapid generation of triplet states: i.e., benzene, naphthalene, anthracene, pyrene, perylene, triphenylene, bromonaphthalene, acetylanthracene, acetone, benzil and biacetyl molecules. First, the geometry optimizations of the structures of these organic molecules were performed using the ωB97XD functional, a dispersion-corrected LC functional, with the cc-pVTZ basis set.[26] Several initial structures were examined for the dimers. Figure 1 displays the optimized structures for both monomers and dimers. The collinear spin-

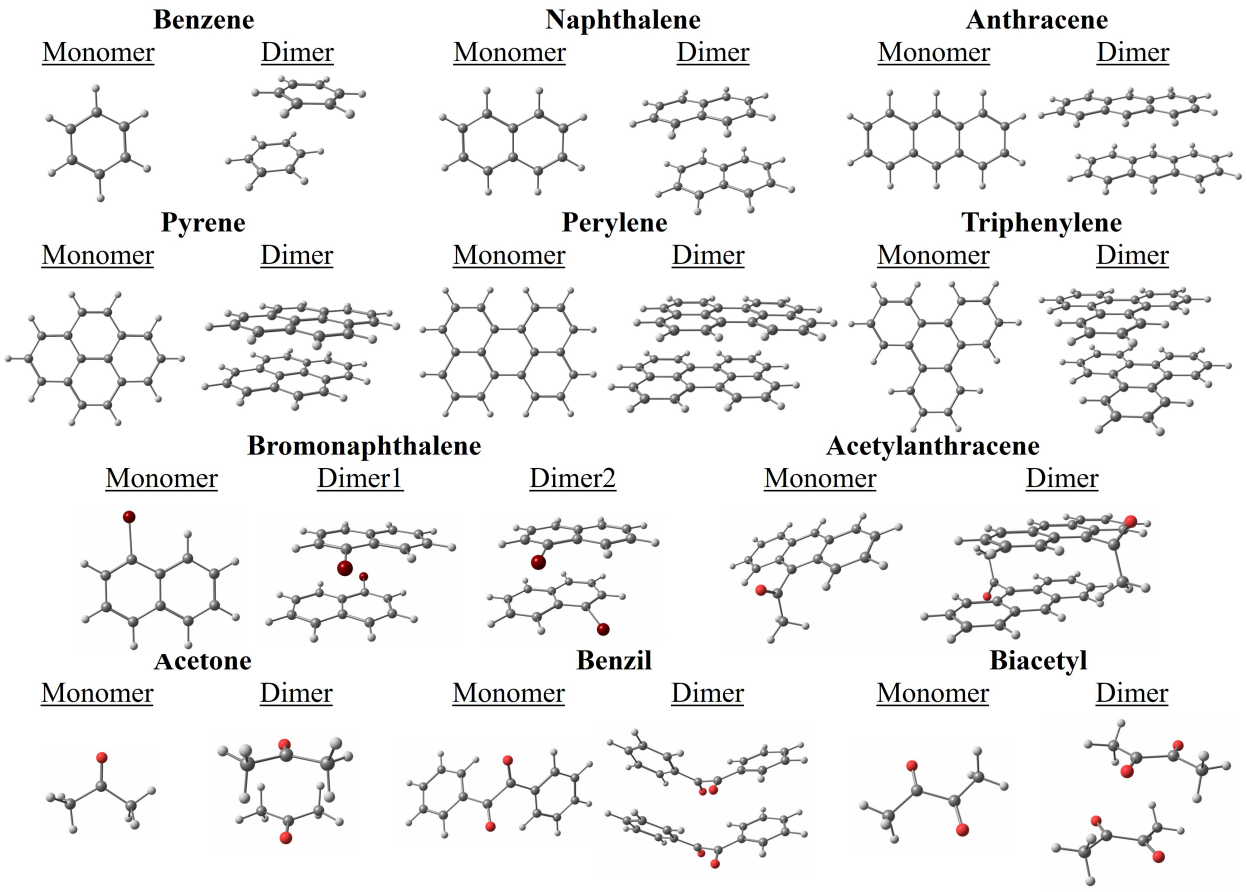

Figure 1: Optimized structures of the calculated organic molecules and their dimers. Geometry optimizations were performed using the ωB97XD functional with the cc-pVTZ basis set. Note that two types of π-stackings are examined only for bromonaphthalene dimer.

flip TDDFT[27,28] calculations with the long-range correction (LC)[29,30] was then performed. In the spin-flip LC-TDDFT calculations, the LC-BLYP functional, combining Becke 1988 exchange[31] with Lee-Yang-Parr correlation,[32] was utilized with the same basis set. Fur-

thermore, TDDFT calculations using the ωB97XD functional (TDωB97XD) were conducted for comparison. Notably, spin-flip LC-TDDFT has demonstrated the capability to accurately predict excitation energies with double excitation effects,[25,33] marking a significant advancement in TDDFT accuracy. In contrast, conventional TDDFT calculations tend to underestimate triplet excitation energies and overestimate singlet excitation energies for photosensitizers.[34] All LC-DFT and LC-TDDFT calculations were carried out using the Gaussian 16 Revision A.03 program,[35] while spin-flip LC-TDDFT calculations were conducted using the development version of the GAMESS program.[36]

First, we categorize heavy atom-free organic molecules into four groups: small acenes (benzene, naphthalene, anthracene), small polycyclic aromatic hydrocarbons (pyrene, perylene, triphenylene), substituted acenes (bromonaphthalene, acetylanthracene), and small ketones (acetone, benzil, biacetyl). Their ISC and SF potentials are assessed using spin-flip LC-TDDFT calculations. For ISC, we focus on two key factors: the energy gap between the S_1 state and the lower triplet state, and adherence to the El-Sayed rule which favors $n\pi^*$ and $\pi\pi^*$ transitions. The study excludes the heavy atom effect as it centers on heavy atom-free molecules. For SF, we consider the energy gap between the $(TT)_1$ state and post-dimerization absorption peaks, the number of states between these peaks and the $(TT)_1$ state, whether the S_1 state is immediately above the $(TT)_1$ state, and their energy gap. The oscillator strengths between the S_0 and S_1 states are evaluated for both ISC and SF. Note that examinations of vibrational spin-orbit couplings and other related aspects are omitted from this study, because the initial process targeted, the formation of the singlet (TT) state, is spin-allowed and occurs substantially faster than spin-orbit coupling. In Tables S1 to S23 of the supporting information, the calculated excitation energies of the spin-flip LC-TDBLYP are compared with the experimental and highly-accurate multiconfiguration results. These tables validate the high accuracy of the calculated excitation energies and also underscore the importance of incorporating double excitation effects into these excitation energy calculations. Based on these criteria, we explore ISC and SF potentials for each molecule type.

We begin our examination by focusing on the mechanisms of triplet generation in small acenes such as benzene, naphthalene, and anthracene. While oligoacenes are well-known molecular systems where SF occurs, these smaller units have been generally overlooked for SF potential despite their capability to generate triplet states. This skepticism stems from the fact that these molecules do not fulfill the traditional criteria for SF progression, particularly conventional condition, which requires the S_1 excitation energy to be more than double the T_1 excitation energy. Furthermore, the singlet-to-triplet conversion rate (k_{ST})

in these molecules is significantly lower than that observed in longer-chain oligoacenes like tetracene and pentacene, where SF is a common occurrence: experimental k_{ST} values being 10^5, 10^6, and 10^8 for benzene, naphthalene, and anthracene, respectively.

Figure 2 illustrates the calculated excitation energy levels for the monomers and π-stacking dimers of benzene, naphthalene, and anthracene. Note that blue arrows indicating

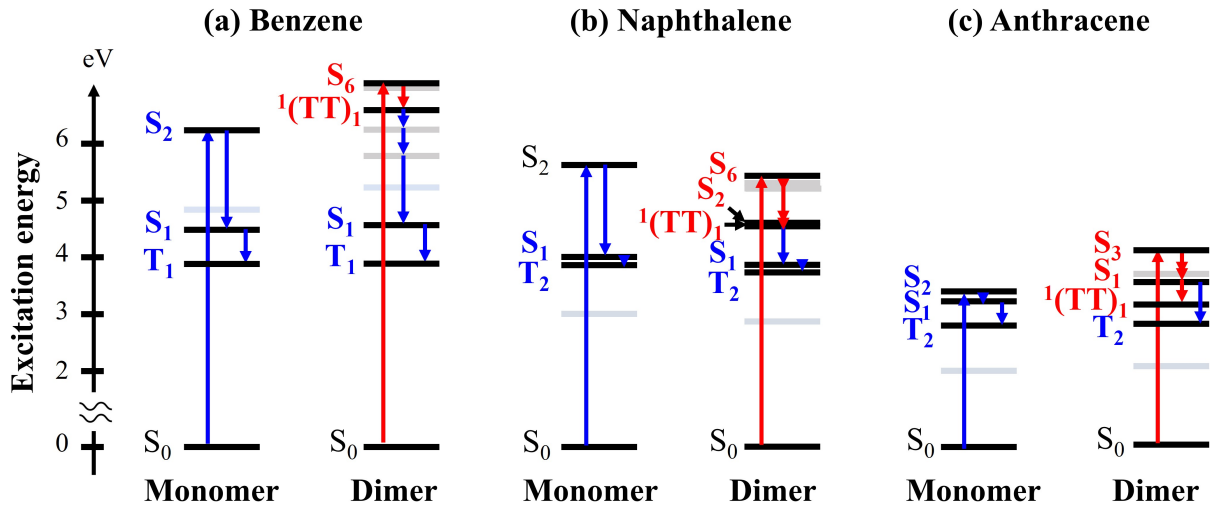

Figure 2: Schematic diagrams of photo-induced state transitions in the monomers and π-stacking dimers of benzene, naphthalene, and anthracene, which integrate calculated spin-flip LC-TDBLYP excitation energies, highlighting the primary transitions that contribute to intersystem crossings in blue and singlet fissions in red. In the diagrams, less contributing singlet and triplet excitations with minimal oscillator strengths are represented by gray and blue gray bars, respectively. The blue arrows indicating state transitions from the ground state (S_0) are only shown when the calculated oscillator strengths are sufficiently large.

state transitions from the ground state (S_0) are only shown when the calculated oscillator strengths are sufficiently large. First, let us explore the potential for ISC in the monomers. The schematic diagrams illustrated with blue arrows in Figs. 2(a) to (c) suggest a lack of correlation between the magnitude of the energy gaps from S_1 excitation to the nearest lower triplet excitations (S-T energy gaps) and the sequence of k_{ST}. The calculated S-T energy gaps, showing no correlation with k_{ST}, are 0.70 eV (T_1), 0.16 eV (T_2), and 0.29 eV (T_2) for benzene, naphthalene, and anthracene monomers, respectively. This lack of correlation is also supported by experimental results showing an inverse relationship with values and by *ab*

initio multireference theories, such as CASPT2 and MRMP, which also demonstrate no such correlation, as shown in Tables S1, S3 and S5. This result is further supported by molecular orbitals composing the main transitions of the excited states involved in the ISC, as shown in Fig. S1 of the supporting information. As evident from these diagrams, all molecular orbitals are pure π orbitals, with no orbitals possessing n-character. This illustrates a departure from the aforementioned El-Sayed rule.

Shifting the focus to the π-stacking dimers of these small acenes, we find a similar trend. Like with the monomers, there is no apparent correlation between the S-T energy gaps and k_{ST}. The S-T energy gaps for the dimers are determined to be 0.68 eV (T_1) for benzene, 0.13 eV (T_2) for naphthalene, and 0.73 eV (T_2) for anthracene, as detailed in Tables S2, S4 and S6. This order does not align with the sequence of k_{ST} at all. Taking into account the results for monomers, the sequence of k_{ST} values does not align logically if the triplet generations are attributed to the progression of ISC. This is further supported by the molecular orbital images in Fig. S2 of the supporting information. These images reveal that the main transitions involve both the source and destination states in $\pi\pi^*$ transitions, violating the El-Sayed rule, albeit with a partial inclusion of charge transfer excitations.

Furthermore, when considering the potential for SF following dimerization, Fig. 2 provides valuable insights. As determined by spin-flip LC-TDBLYP calculations, the absorption peaks marked by the tips of the red arrows correspond to specific excitations: S_6 for benzene, S_6 for naphthalene, and S_3 for anthracene. The experimental absorption peaks in the UV-Vis spectra align closely with these excitation energies. Importantly, the $^1(\mathrm{TT})_1$ excitation, which triggers SF, exists in the energy region just below these absorption peaks. This indicates that SF is likely to proceed easily. However, for benzene and naphthalene dimers, the possibility of skipping the $^1(\mathrm{TT})_1$ state during de-excitation is high, which may contribute to the observed order of k_{ST}. In the case of anthracene dimer, it is crucial to note that the $(\mathrm{TT})_1$ excitation lies just below the absorption peak of the S_1 excitation, suggesting a high probability of spin-allowed de-excitation to the $^1(\mathrm{TT})_1$ state and thus leading to a high k_{ST}.

This could explain the discrepancy between the calculated energy gaps and the experimental k_{ST} values. Therefore, while singlet-to-triplet conversion via ISC shows no correlation with k_{ST}, the scenario changes when considering SF progression. The findings imply that SF progression, a common feature in longer-chain oligoacenes, could also be a viable mechanism in these smaller acene molecules. This analysis provides a more comprehensive understanding of the photophysical behaviors of small acenes and their potential in SF applications.

SF progression has been extensively studied and reported in molecular systems with one-dimensional extension.[12] This raises an intriguing question: Is SF feasible in molecular systems that extend two-dimensionally? To explore this, we focus on the potential for SF in small polycyclic aromatic hydrocarbons (PAHs), such as pyrene, perylene, and triphenylene, which resemble small graphene flakes. Notably, these small PAHs, even without heavy atoms, are capable of generating triplet states under light irradiation, with experimental k_{ST} values for pyrene, perylene, and triphenylene (10^6, $<10^8$, and 5×10^7, respectively) indicating significant triplet generation.[1]

Initially, we consider the potential for ISC in the monomers of these small PAHs. Figure 3 summarizes the calculated results for critical excitations involved in the ISCs for both the monomers and π-stacking dimers of pyrene, perylene, and triphenylene. The accuracy of the calculated energy levels aligns well with the reference CASPT2 calculation results, offering excitation energies that are remarkably similar, as shown in Tables S7, S9, and S11 of the supporting information. For the monomers, the S-T energy gaps obtained from spin-flip LC-TDBLYP calculations are substantial: 0.37 eV (T_2) for pyrene, 0.92 eV (T_2) for perylene, and 0.51 eV (T_1) for triphenylene. The order of these energy gap values is the opposite of the experimental results for k_{ST}, which increase in the sequence of perylene, triphenylene, and pyrene, contradicting the conventional view that triplet generation is driven by ISC. This finding is consistent with the El-Sayed rule, examined in the context of the molecular orbitals in Fig. S3 of the supporting information. As evident from these depictions, all excitations in these monomers are $\pi\pi^*$ transitions, with no localized n orbitals in any molecular orbital.

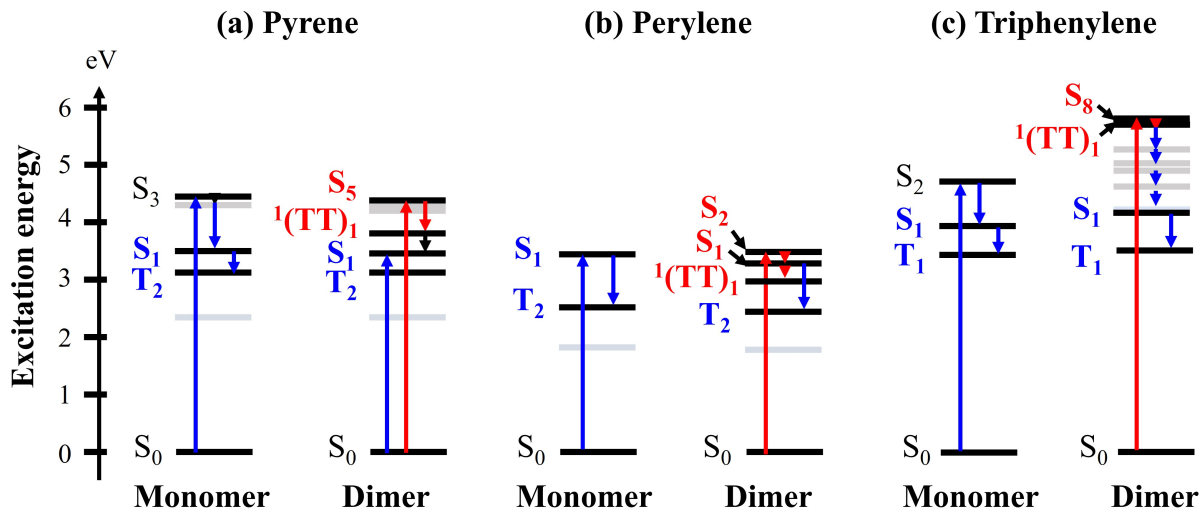

Figure 3: Schematic diagrams of photo-induced state transitions in the monomers and π-stacking dimers of pyrene, perylene and triphenylene, which integrate calculated spin-flip LC-TDBLYP excitation energies, highlighting the primary transitions that contribute to intersystem crossings in blue and singlet fissions in red. In the diagrams, less contributing singlet and triplet excitations with minimal oscillator strengths are represented by gray and blue gray bars, respectively. The blue arrows indicating state transitions from the ground state (S_0) are only shown when the calculated oscillator strengths are sufficiently large.

Thus, the ISC in these molecules does not adhere to the El-Sayed rule, leading to the conclusion that the possibility of ISC progression is extremely low, even considering the large S-T energy gaps.

We extend our investigation to the π-stacking dimers of these small PAHs. Figure 3 includes schematic diagrams related to triplet generation in small PAH dimers. These diagrams indicate that the calculated S-T energy gaps, 0.34 eV (T_2) for pyrene, 0.84 eV (T_2) for perylene, and 0.66 eV (T_1) for triphenylene as detailed in Tables S8, S10 and S12, still display an inverse correlation with k_{ST}, although slightly smaller than those for monomers. As shown in Fig. S4 of the supporting information, the molecular orbitals forming the main transitions, involving the S_1 excitation and immediately lower triplet excitations contributing to ISC, adhere to the El-Sayed rule. Specific excitations demonstrate electron transferability, indicating the need for long-range correction in TDDFT. However, none of these excitations explicitly include $n\pi^*$ transitions with localized n orbitals, leading to the conclusion that the

possibility of ISC progression in small PAH dimers is also extremely low.

Lastly, we turn our attention to the potential for SF progression in these small PAH dimers. From Figs. 3, the high-absorption peaks correspond to specific excitations for each dimer: S_5 excitation for pyrene dimer, S_2 excitation for perylene dimer, and S_8 excitation for triphenylene dimer. The calculated energy gaps between these absorption peaks and the $^1(TT)_1$ excitation, obtained using spin-flip LC-TDBLYP, vary across the dimers: 0.57 eV for pyrene, 0.51 eV for perylene, and 0.11 eV for triphenylene. For pyrene, the S_1 excitation, with high absorption, is expected to be lower than the $^1(TT)_1$ one, facilitating bypassing of de-excitation to the $^1(TT)_1$ state through direct de-excitations. The de-excitation of perylene likely occurs via the S_1 state, which is close to the $^1(TT)_1$ excitation, suggesting a high likelihood of SF progression. In the case of triphenylene, characterized by a narrow energy gap between its absorption peak and the $^1(TT)_1$ excitation, the likelihood of SF progression is limited due to the high probability of bypassing the $^1(TT)_1$ excitation during de-excitation, a result of the many states surrounding this excitation. Based on these findings, the SF progression probability is expected to follow the order of perylene, triphenylene, and pyrene, explaining the order of k_{ST}. This result supports the SF progression in these small PAHs.

Next, let us next delve into how the introduction of substituents impacts the potential for SF progression in the triplet generation of organic molecules. While the addition of heavy atom groups to molecules is often thought to lead to faster triplet generation due to enhanced spin-orbit coupling effects, this is not always the case. In some instances, the introduction of such groups does not accelerate, or even decelerates, the triplet generation process. Contrarily, in certain cases, substituents can dramatically increase the rate of triplet generation. This is exemplified by the high experimental k_{ST} values for bromonaphthalene and acetylanthracene, which demonstrate the significant impact of substituents.

To comprehend these phenomena, we first focus on bromonaphthalene and acetylanthracene monomers. These molecules show a marked enhancement in triplet generation when bromo and acetyl groups are added, respectively. We explore this effect through an ex-

amination of ISC in the monomers of these substituted acenes. Figure 4 compiles calculated results for the excitations involved in ISC for both the monomers and π-stacking dimers of these molecules. The figure illustrates that the sequence of the S-T energy gaps inversely

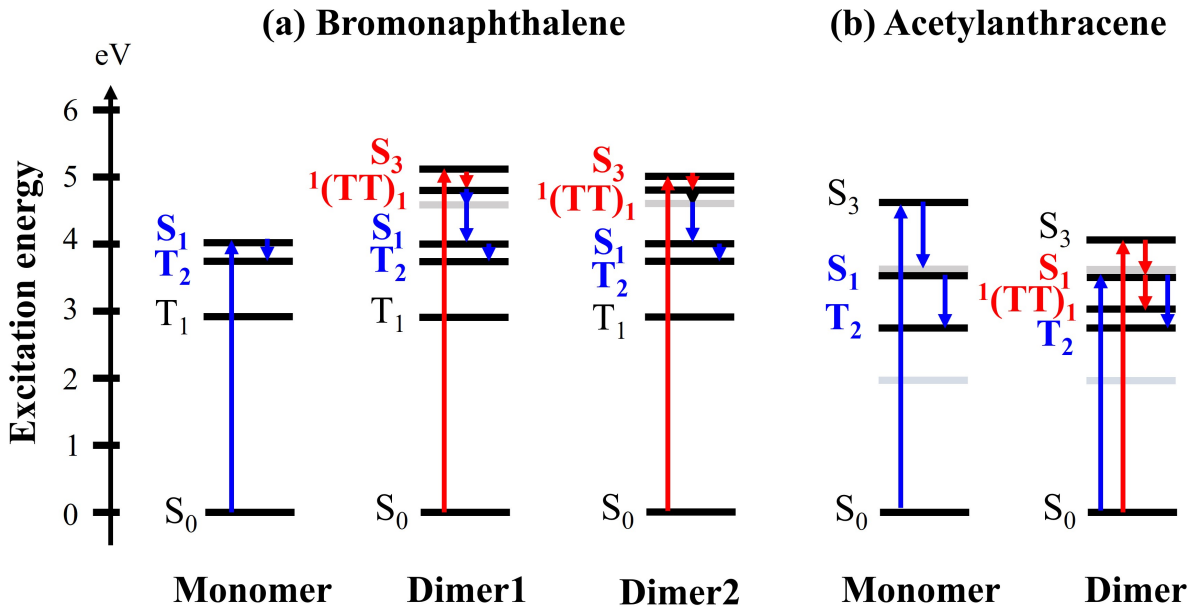

Figure 4: Schematic diagrams of photo-induced state transitions in the monomers and π-stacking dimers of bromonaphthalene and acetylanthracene, which integrate calculated spin-flip LC-TDBLYP excitation energies, highlighting the primary transitions that contribute to intersystem crossings in blue and singlet fissions in red. In the diagrams, less contributing singlet and triplet excitations with minimal oscillator strengths are represented by gray and blue gray bars, respectively. The blue arrows indicating state transitions from the ground state (S_0) are only shown when the calculated oscillator strengths are sufficiently large.

correlates with k_{ST} values for the monomers, specifically, 0.27 eV (T_2) for bromonaphthalene and 0.78 eV (T_2) for acetylanthracene (see Tables S13 and S16 for the energy values). Note, however, that the S_1 excitation of acetylanthracene significantly differs from the absorption peak value in the experimental UV-Vis spectrum, suggesting that the actual S-T energy gap for the acetylanthracene monomer might be considerably smaller than calculated. Therefore, both substituted acenes could have energy gaps that do not impede ISC progression. When considering the El-Sayed rule, these monomers exhibit a discrepancy. As depicted in Fig. S5 of the supporting information, the molecular orbital compositions of the main transitions

involving T_2 and S_1 excitations related to ISC in bromonaphthalene include transitions from localized n orbitals in the bromine group to π^* orbitals, partially adhering to the El-Sayed rule. However, in acetylanthracene, all transitions are $\pi\pi^*$, indicating a lower probability of ISC progression.

Turning our attention to the dimers, we found that the S-T energy gaps for bromonaphthalene dimers are relatively small, while those for acetylanthracene dimers are larger: 0.26 eV (T_2) for dimer 1, 0.27 eV (T_2) for dimer 2. and 0.75 eV (T_2) for bromonaphthalene dimer 1 and dimers and acetylanthracene dimer, respectively, as shown in Tables S14, S15 and S17. This difference in energy gaps may influence the trend in k_{ST} values for acetylanthracene dimers. According to Fig. S6 of the supporting information, the molecular orbitals associated with the main transitions in ISC for bromonaphthalene dimers, containing heavy atoms, are predominantly $\pi\pi^*$ type. However, they also feature molecular orbitals with n orbitals localized on bromine atoms. This characteristic demonstrates a partial compliance with the El-Sayed rule and implies a potential for slow ISC progression. In contrast, acetylanthracene dimers exhibit a slightly different molecular orbital composition compared to their monomers. Figure S6 shows that there is a minor contribution of $n\pi^*$ transition in the S_1 excitation for acetylanthracene dimers. This partial adherence to the El-Sayed rule indicates a possibility of ISC progression, but the large energy gap suggests that the rate of ISC progression would be considerably slow.

For SF progression in substituted acene dimers, Fig. 4 reveals that both bromonaphthalene dimers and the acetylacetone dimer exhibit S_3 excitations. The $(TT)_1$ excitation for bromonaphthalene dimers is just below the absorption peak S_3, with energy gaps of 0.32 eV for dimer 1 and 0.22 eV for dimer 2. This positioning indicates a potential for rapid SF progression. However, the presence of S_1 and S_2 excitations below the $(TT)_1$ excitation in these dimers raises the likelihood of bypassing the $(TT)_1$ state during de-excitation. Considering the high probability of progressing to the S_1 excitation, it is anticipated that ISC to the T_2 state would also occur at a notable rate in these scenarios. For the acetylanthracene dimer,

S_1 and S_2 excitations lie between the absorption peak and the $(TT)_1$ excitation. Given that the $(TT)_1$ excitation is situated below the S_1 state, de-excitation is expected to proceed until reaching the S_1 excitation. The small oscillator strength between the S_1 and S_0 states, as shown in Table S17, implies a prolonged lifetime in the S_1 excitation before transitioning to the $(TT)_1$ excitation. A key aspect for the acetylanthracene dimer is the potential presence of a peak corresponding to the $^1(TT)_1$ excitation in the UV-Vis spectrum. The absence of a corresponding excitation peak to the 2.82 eV value in both the monomer and dimer of acetylanthracene suggests a direct SF progression, which could explain the large k_{ST} observed.

We also investigate whether singlet fission (SF) progression is exclusively associated with π-stacking or applicable to dimerizing systems as well. In conventional studies on SF, the focus so far has been primarily on systems that form π-stacking dimers.[12] However, some molecules, which do not typically form π-stacking structures, still efficiently generate triplet states. A key example of this phenomenon is observed in small ketones like acetone, benzil, and biacetyl. Despite their structural characteristics not being particularly conducive to dimerization, these small ketones demonstrate higher rates of triplet state formation compared to small acenes. This is reflected in their experimental k_{ST} values, which are 5×10^8, 5×10^8 and 7×10^7 for acetone, benzil and biacetyl, respectively.[1] Traditional explanations for the triplet state formation in these ketones have centered around ISC using $n\pi^*$ transitions involving the n orbital of oxygen, but without specific verification.

To better understand the underlying mechanisms, we examine the possibility of ISC progression in small ketone monomers and the role of SF in triplet state generation more broadly. Figure 5 summarizes computational results related to excitations involved in the triplet state generation for monomers and dimers of acetone, benzil, and biacetyl. For the monomers, the spin-flip LC-TDBLYP calculations for the S-T energy gaps are significant: 1.43 eV (T_1) for acetone, 0.73 eV (T_1) for benzil, and 0.96 eV (T_1) for biacetyl (for the energy values, see Tables S18, S20, and S22). These calculated gaps also do not seem to

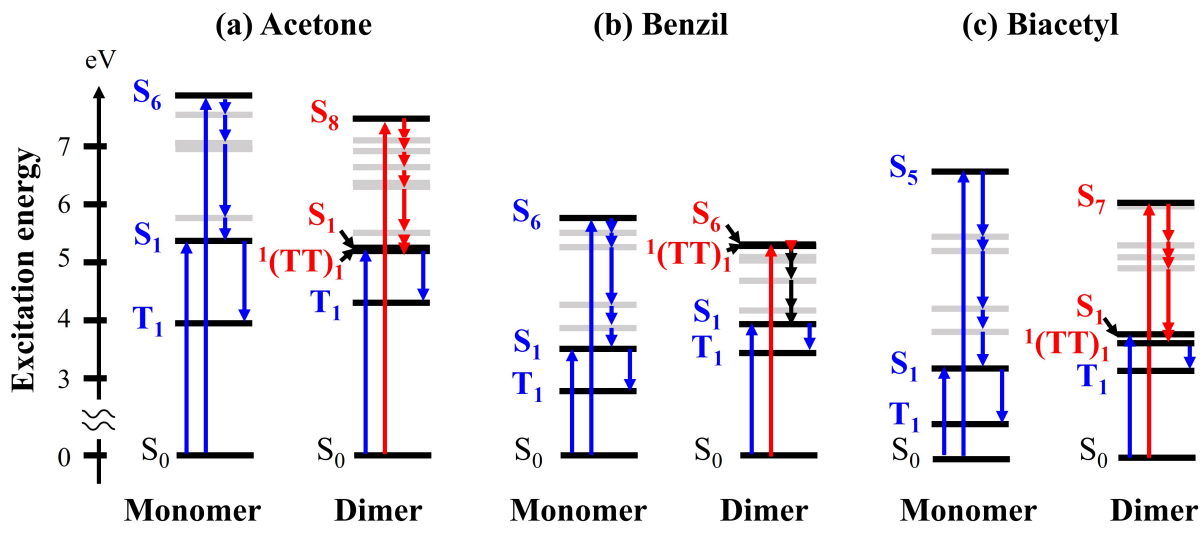

Figure 5: Schematic diagrams of photo-induced state transitions in the monomers and dimers of acetone, benzil and biacetyl, which integrate calculated spin-flip LC-TDBLYP excitation energies, highlighting the primary transitions that contribute to intersystem crossings in blue and singlet fissions in red. In the diagrams, less contributing singlet and triplet excitations with minimal oscillator strengths are represented by gray and blue gray bars, respectively. The blue arrows indicating state transitions from the ground state (S_0) are only shown when the calculated oscillator strengths are sufficiently large.

correlate with the order of k_{ST} values. Furthermore, the molecular orbitals in Fig. S7 of the supporting information show that the main transitions of the S_1 excitation and the immediate triplet excitation for each molecule are composed of molecular orbitals of the same shape, indicating that ISC inherently involves transitions between excitations of the same character. This finding implies that ISC is less likely to proceed in these small ketone monomers, as they do not follow the El-Sayed rule.

Focusing on small ketone dimers, the calculated S-T energy gaps for the excitations involved in ISC are also considerable. Figure 5 illustrates a notable distinction in excitation energies between monomers and dimers, a contrast to the behavior observed in molecules that undergo dimerization via π-stacking. On the other hand, the calculations show considerable S-T energy gaps for acetone, benzil, and biacetyl dimers, similar to their monomer counterparts: 1.42 eV (T_1) for acetone, 0.75 eV (T_1) for benzil, and 0.95 eV (T_1) for biacetyl (for the energy values, see Tables S19, S21, and S23). These values do not align with the

order of k_{ST} and are relatively large. However, like the monomers, these excitation energies might differ from experimental results, prompting a closer look at whether they adhere to the El-Sayed rule. In the case of acetone dimer, the main transitions of the S_1 excitation and the underlying T_1 excitation involve different destination molecular orbitals compared to the monomer as shown in Fig. S8. This divergence occurs because the order of T_2 and S_1 is reversed in the dimer compared to the monomer. As a result, the T_1 excitation involves an $n\pi^*$ transition, while the S_1 excitation involves a $\pi\pi^*$ transition, increasing the likelihood of ISC progression in the acetone dimer. For benzil and biacetyl dimers, however, even in the dimer form, the S_1 excitation and the underlying T_1 excitation are composed of the same transitions, which indicates a lower likelihood of ISC progression. Therefore, the order of k_{ST} cannot be fully explained by ISC alone in these cases.

In addition to ISC, we also consider the potential for SF progression in small ketone dimers that do not involve π-stacking. According to Fig. 5, the $(TT)_1$ excitations are situated just below the S_1 excitations, with minimal energy gaps: 0.08 eV for acetone dimer, 0.03 eV for benzil dimer, and 0.23 eV for biacetyl dimer as shown in Tables S19, S21 and S23. Given the near-zero oscillator strengths of the S_1 excitations, these states have prolonged lifetimes, increasing the likelihood of transitioning to the $^1(TT)_1$ excited state rather than returning to the S_0 ground state. This high probability suggests that SF progression is very likely in these small ketone dimers. However, the location of strong absorption peaks at higher energy levels, such as S_8 for the acetone dimer, S_6 for the benzil dimer, and S_7 for the biacetyl dimer, could mean that relaxation to the S_1 excitation may take time, potentially affecting the rate of SF progression. The notably high k_{ST} values for acetone and biacetyl may be attributed to the minimal energy gaps between the $(TT)_1$ and S_1 states, which are 0.08 eV for acetone and 0.23 eV for biacetyl dimers, respectively. Following relaxation to the S_1 state, a rapid transition to the $^1(TT)_1$ state is anticipated. These results show that these small ketone dimers have a high likelihood of undergoing SF progression despite not forming π-stacking. Nevertheless, due to the elevated energy levels of the absorption peaks,

the relaxation process could be time-consuming, impacting the efficiency of SF progression.

Overall, our findings indicate that while π-stacking is a common feature in molecules exhibiting efficient SF, it is not an absolute requirement. Small ketone dimers, which do not typically form π-stacking structures, still demonstrate a high potential for SF progression. However, the detailed dynamics of the relaxation process and the specific characteristics of the molecular orbitals involved play a crucial role in determining the efficiency and likelihood of SF progression in these systems.

Based on the above findings that support the role of SF in triplet generation, it becomes imperative to explore the extent to which the variations in triplet generation rates (k_{ST}) across different organic molecules can be thoroughly attributed to SF mechanisms. To achieve this, it is essential to correlate k_{ST} with various factors that significantly affect the progression of SF and ISC. In our discussion regarding the possibilities of SF progression, particularly in dimers, we focus on five key factors: the energy gap between the $(\mathrm{TT})_1$ state and the higher-energy absorption peak ($\Delta E_{\mathrm{abs-(TT)}}$), the singlet state corresponding to that absorption peak ($\mathrm{S_{abs}}$), the singlet state just above the $(\mathrm{TT})_1$ state ($\mathrm{S_{>(TT)}}$), the energy gap between the $(\mathrm{TT})_1$ and the S_1 states ($\Delta E_{\mathrm{S1-(TT)}}$), and the oscillator strength of the S1 excitation in dimers ($f_{\mathrm{S1}}^{\mathrm{dimer}}$). Conversely, when discussing the potential for ISC progression, particularly in monomers, we consider factors such as the energy gap between the triplet and the S_1 states ($\Delta E_{\mathrm{S1-T}}$), compliance with the El-Sayed rule, and the oscillator strength of the S_1 excitation in monomers ($f_{\mathrm{S1}}^{\mathrm{monomer}}$). Table 1 summarizes the key descriptors related to singlet fission and intersystem crossing for the dimers and monomers of eleven heavy atom-free organic molecules, arranged in ascending order of k_{ST}. As seen in the table, SF-related factors, particularly $\Delta E_{\mathrm{abs-(TT)}}$ and the presence of the S_1 state in $\mathrm{S_{>(TT)}}$, demonstrate a strong correlation with the order of k_{ST}. This is further emphasized by underlining values of $\Delta E_{\mathrm{abs-(TT)}}$ and $\Delta E_{\mathrm{S1-(TT)}}$ below 0.25 eV and instances where $\mathrm{S_{>(TT)}}$ is S_1 in the table, indicating their strong relation with k_{ST}. The general trend aligns with smaller $\Delta E_{\mathrm{abs-(TT)}}$ and $\Delta E_{\mathrm{S1-(TT)}}$ values and instances where $\mathrm{S_{>(TT)}}$ is S_1, except for specific cases like triphenylene

and acetylanthracene, though constructing a data science model focused on k_{ST} as the target variable requires more data. In triphenylene dimer, the absorption peak is at the S_8 excitation, with the $(TT)_1$ excitation between the S_6 and S_7 excitations, both at higher energy levels. The presence of the S_7 excitation and S_1 to S_6 excitations below the $(TT)_1$ excitation suggests a high likelihood of skipping the $(TT)_1$ excitation during relaxation. For acetylanthracene dimer, the absorption peak at the $^1(TT)_1$ excitation potentially contributes to its large k_{ST}, as absorption at this excitation facilitates direct SF progression without needing relaxation from other absorption peaks. Regarding ISC, the descriptors, particularly ΔE_{S1-T} and adherence to the El-Sayed rule, exhibit little correlation with k_{ST} order. Furthermore, both monomers and dimers mostly lack molecules with a high likelihood of ISC progression. TT annihilation, the reverse reaction of SF, has been experimentally confirmed for all the molecules studied as described above, further cementing SF as the primary mechanism for triplet generations in these organic molecules.

To summarize the results, the sequence of descriptors influencing the acceleration of triplet generation rates in heavy atom-free organic molecules is proposed as follows:

1. SF: Absorption peak at $^1(TT)_1$ excitation: Molecules exhibiting absorption at the $(TT)_1$ excitation show rapid triplet generation.

2. SF: Energy gap between S_1 and $^1(TT)_1$ excitations: Narrower gaps between the S_1 and $^1(TT)_1$ excitations facilitate more rapid generation of triplet states in dimers.

3. SF: Energy gap between absorption peak and $^1(TT)_1$ excitation: A smaller energy gap between the absorption peak and the $(TT)_1$ excitation leads to even quicker triplet state generation in dimers.

4. SF: Singlet state density above and below $(TT)_1$ excitation: A lower number of singlet states intervening between the absorption peak and the S_1 excitation accelerates triplet state formation. In particular, fewer singlet states below the $(TT)_1$ excitation lead to faster generation of triplet states.

5. SF: Immediate placement of S_1 excitation above $^1(TT)_1$: The proximity of the S_1 excitation right above the $(TT)_1$ level enhances the efficiency of de-excitation to the $(TT)_1$ state, thus expediting triplet state generation.

6. SF: Oscillator strength of the S_1 excitation: When the S_1 excitation lies directly above the $(TT)_1$ level, a diminished oscillator strength for the S_1 transition contributes to more effective de-excitation to the $^1(TT)_1$ state.

7. ISC: Compliance with the El-Sayed rule: Adherence to the El-Sayed rule, which favors certain transitions, predicts the likelihood of ISC processes.

8. ISC: Energy gap between the S_1 state and the nearest triplet state: Narrower energy gaps between the S_1 state and the closest lower triplet state tend to facilitate quicker ISC events.

Determining whether triplet generation in experiments results from SF or ISC based on yield data is challenging; however, observing time-resolved photoluminescence is likely the most effective method for distinguishing between these processes.[37]

Table 1: Descriptors for dimers and monomers of eleven heavy atom-free organic molecules linked to singlet fission (SF) and intersystem crossing (ISC), respectively, including experimental values of the singlet-to-triplet conversion rate, k_{ST}. For SF, factors comprise the energy gap between the $(\mathrm{TT})_1$ state and the next higher-energy absorption peak, $\Delta E_{\mathrm{abs-(TT)}}$, the specific singlet state of that absorption peak, $\mathrm{S_{abs}}$, the singlet state immediately above the $(\mathrm{TT})_1$ state, $\mathrm{S_{>(TT)}}$, the energy gap between the $(\mathrm{TT})_1$ and the $\mathrm{S_1}$ states, $\Delta E_{\mathrm{S1-(TT)}}$, and the oscillator strength for the $\mathrm{S_1}$ excitation, $f_{\mathrm{S1}}^{\mathrm{dimer}}$. For ISC, factors include the energy gap between the triplet and the $\mathrm{S_1}$ states, $\Delta E_{\mathrm{S1-T}}$, to assess compliance with the El-Sayed rule, and the oscillator strength of the $\mathrm{S_1}$ excitation, $f_{\mathrm{S1}}^{\mathrm{monomer}}$. All energy values are presented in eV units. $\Delta E_{\mathrm{abs-(TT)}}$ below 0.25 eV, the $\mathrm{S_1}$ state in $\mathrm{S_{>(TT)}}$ and $\Delta E_{\mathrm{S1-(TT)}}$ under 0.25 eV are underlined to emphasize their correlation with k_{ST}.

		Singlet fission					Intersystem crossing		
Molecules	$k_{\mathrm{ST}}{}^{(a)}$	$\Delta E_{\mathrm{abs-(TT)}}$	$\mathrm{S_{abs}}$	$\mathrm{S_{>(TT)}}$	$\Delta E_{\mathrm{S1-(TT)}}$	$f_{\mathrm{S1}}^{\mathrm{dimer}}$	$\Delta E_{\mathrm{S1-T}}$	El-Sayed	$f_{\mathrm{S1}}^{\mathrm{monomer}}$
Benzene	10^5	0.47	$\mathrm{S_6}$	$\mathrm{S_4}$	−2.02	0.0029	0.70	No	0.0000
Naphthalene	10^6	0.89	$\mathrm{S_6}$	$\mathrm{S_2}$	−0.68	0.0008	0.16	No	0.0001
Pyrene	10^6	0.57	$\mathrm{S_5}$	$\mathrm{S_2}$	−0.35	0.1921	0.37	No	0.0014
Triphenylene	5×10^7	<u>0.11</u>	$\mathrm{S_8}$	$\mathrm{S_7}$	−1.53	0.0001	0.51	No	0.0000
Biacetyl	7×10^7	3.61	$\mathrm{S_7}$	<u>$\mathrm{S_1}$</u>	<u>0.23</u>	0.0001	0.96	No	0.5456
Perylene	$<10^8$	0.51	$\mathrm{S_2}$	<u>$\mathrm{S_1}$</u>	0.31	0.0000	0.92	No	0.0001
Anthracene	10^8	0.95	$\mathrm{S_3}$	<u>$\mathrm{S_1}$</u>	0.56	0.0000	0.75	No	0.0010
Acetone	5×10^8	3.42	$\mathrm{S_8}$	<u>$\mathrm{S_1}$</u>	<u>0.08</u>	0.0379	1.43	No	0.0379
Benzil	5×10^8	<u>0.03</u>	$\mathrm{S_6}$	$\mathrm{S_6}$	−1.89	0.0005	0.73	No	0.0005
Bromonaphthalene	10^9	<u>0.22</u>	$\mathrm{S_3}$	$\mathrm{S_3}$	−0.80	0.0014	0.27	Yes	0.0014
Acetylanthracene$^{(b)}$	$\sim10^{10}$	1.01	$\mathrm{S_3}$	<u>$\mathrm{S_1}$</u>	0.48	0.0012	0.78	No	0.0012
Benzophenone$^{(b,c)}$	10^{11}	<u>0.14</u>	$\mathrm{S_4}$	$\mathrm{S_8}$	−1.99	0.0096	1.00	Yes	0.0012

(a) Ref.[1] . (b) The absorption peaks are anticipated for the $^1(\mathrm{TT})_1$ excitations. (c) Ref.[21] .

In conclusion, we have explored the triplet generation mechanisms of heavy atom-free organic molecules by comparing the effective factors contributing to singlet fissions (SFs) and intersystem crossings (ISCs). We have consequently revealed that SF is the predominant route for the triplet generations.

In this study, we have examined the triplet generation mechanisms of 11 types of organic molecules from the perspectives of ISC and SF progression possibilities. These molecules included small acenes that extend in one dimension such as benzene, naphthalene, and anthracene; small polycyclic aromatic hydrocarbons that extend in two dimensions like pyrene, perylene, and triphenylene; substituted acenes with substituents such as bromonaphthalene and acetylanthracene; and small ketones forming dimers not involving π-stacking like acetone, benzil, and biacetyl. As a result, no correlation was found between the triplet generation rates and factors considered to influence ISC progression, such as the energy gap between the triplet and the S_1 states, or compliance with the El-Sayed rule. On the other hand, the magnitude of triplet generation rates was found to be strongly correlated with factors influencing SF progression, such as the energy gap between the $(TT)_1$ state and the higher-energy absorption peak, and the singlet state just above the $(TT)_1$ state. This leads to the conclusion that SF initiates the triplet generations in heavy atom-free organic molecules. This conclusion is consistent with the experimental observation of triplet-triplet annihilations, which are the reverse reaction of SF, in all these molecules.

Based on the above results, the conditions for SF progression are updated as follows:

1. There is a high-absorption singlet state just above the triplet-triplet excitation of chromophore dimer, or the triplet-triplet excitation itself corresponds to an absorption peak, and

2. the dimerization energy of chromophores is moderately above the solvation energy.

Under these conditions, the rate of SF progression is ranked in the following order:

1. SF occurs most rapidly when the $(TT)_1$ excitation itself corresponds to an absorption

peak.

2. If the $(TT)_1$ excitation does not align with an absorption peak, a high rate of SF is still achieved when an absorption peak is located directly above the $(TT)_1$ excitation.

3. Even with a gap between the absorption peak and the $(TT)_1$ excitation, SF can proceed at a relatively fast rate provided the S_1 excitation is positioned immediately above the $(TT)_1$.

These conditions are met by all organic molecules that generate triplet states rapidly, as far as we know.

Acknowledgments

This research was financially supported by JST CREST, Japan (Grant No. JPMJCR1902).

Supporting Information Available

In Tables S1 to S23, the calculated excitation energies of 11 organic molecules are compiled for their monomers and dimers. Figures S1 to S8 show the molecular orbitals constituting the main transitions involved in ISC for the monomers and SF for the dimers.

Data availability

All data generated or analyzed during this study are included in this published article and its supplementary information files but are available from the corresponding author upon reasonable request.

Figure Captions

Fig. 1. Optimized structures of the calculated organic molecules and their dimers. Geometry optimizations were performed using the ωB97XD functional with the cc-pVTZ basis set. Solvent effects were not considered in the optimizations.

Fig. 2. Schematic diagrams of photo-induced state transitions in the monomers and π-stacking dimers of benzene, naphthalene, and anthracene, which integrate calculated spin-flip LC-TDBLYP excitation energies, highlighting the primary transitions that contribute to intersystem crossings in blue and singlet fissions in red. In the diagrams, less contributing singlet and triplet excitations with minimal oscillator strengths are represented by gray and blue gray bars, respectively. The blue arrows indicating state transitions from the ground state (S_0) are only shown when the calculated oscillator strengths are sufficiently large.

Fig. 3. Schematic diagrams of photo-induced state transitions in the monomers and π-stacking dimers of pyrene, perylene and triphenylene, which integrate calculated spin-flip LC-TDBLYP excitation energies, highlighting the primary transitions that contribute to intersystem crossings in blue and singlet fissions in red. In the diagrams, less contributing singlet and triplet excitations with minimal oscillator strengths are represented by gray and blue gray bars, respectively. The blue arrows indicating state transitions from the ground state (S_0) are only shown when the calculated oscillator strengths are sufficiently large.

Fig. 4. Schematic diagrams of photo-induced state transitions in the monomers and π-stacking dimers of bromonaphthalene and acetylanthracene, which integrate calculated spin-flip LC-TDBLYP excitation energies, highlighting the primary transitions that contribute to intersystem crossings in blue and singlet fissions in red. In the diagrams, less contributing singlet and triplet excitations with minimal oscillator strengths are represented by gray and blue gray bars, respectively. The blue arrows indicating state transitions from the ground state (S_0) are only shown when the calculated oscillator strengths are sufficiently large.

Fig. 5. Schematic diagrams of photo-induced state transitions in the monomers and dimers of bromonaphthalene and acetylanthracene, which integrate calculated spin-flip LC-TDBLYP excitation energies, highlighting the primary transitions that contribute to intersystem crossings in blue and singlet fissions in red. In the diagrams, less contributing singlet and triplet excitations with minimal oscillator strengths are represented by gray and blue gray bars, respectively. The blue arrows indicating state transitions from the ground state (S_0) are only shown when the calculated oscillator strengths are sufficiently large.

References

(1) Turro, N. J., Ramamurthy, V., Scaiano, J. C., Eds. *Principles of Molecular Photochemistry*; University Science Books, Herndon, 2009.

(2) El-Sayed, M. A. The Radiationless Processes Involving Change of Multiplicity in the Diazenes. *J. Chem. Phys.* **1962**, *36*, 573–574.

(3) Yabumoto, S.; Sato, S.; Hamaguchi, H. Vibrational and Electronic Infrared Absorption Spectra of Benzophenone in the Lowest Excited Triplet State. *Chem. Phys. Lett.* **2005**, *416*, 100–103.

(4) McGlynn, S. P.; Azumi, T.; Kasha, M. External HeavyAtom Spin-Orbital Coupling Effect. V. Absorption Studies of Triplet States. *J. Chem. Phys.* **2004**, *40*, 507–515.

(5) Gastilovich, E. A.; Klimenko, V. G.; Korol'kova, N. V.; Nurmukhametov, R. N. Effect of a Heavy Atom in the $S_1(\pi\pi^*)\rightarrow T_1(\pi\pi^*)$ Nonradiative Transition. 9,10-Dichloroanthracene. *Opt. Spectrosc.* **2008**, *105*, 489–495.

(6) Dreeskamp, H.; Koch, E. FFluorescence of Bromoperylenes and TFE Requirements of Heavy-Atom Quenching. *Chem. Phys. Lett.* **1975**, *31*, 251–253.

(7) Halpern, A. M.; Ware, W. R. Luminescent Properties of Hexafluoroacetone. III. Vibrational Relaxation and Radiationless Processes in the Gas Phase. *J. Chem. Phys.* **2003**, *53*, 1969–1977.

(8) Almgren, M. Triplet Yield and Fluorescence Lifetime of Biacetyl in Aqueous Solution. *Mol. Photochem.* **1970**, *4*, 327–334.

(9) Montero, R.; Martinez-Martinez, V.; Longarte, A.; Epelde-Elezcano, N.; Lamas, I.; nigo López Arbeloa, I. Viewpoint Regarding Singlet Fission Mediated Photophysics of BODIPY Dimers. *J. Phys. Chem. Lett.* **2021**, *12*, 7439–7441.

(10) Parker, D. S. N.; Minns, R. S.; Penfold, T. J.; Worth, G. A.; Fielding, H. H. Ultrafast Dynamics of the S1 Excited State of Benzene. *Chem. Phys. Lett.* **2009**, *469*, 43–47.

(11) Perumal, S.; Minaev, B.; Agren, H. Spin-Spin and Spin-Orbit Interactions in Nanographene Fragments: A Quantum Chemistry Approach. *J. Chem. Phys.* **2012**, *136*, 104702(1–16).

(12) Smith, M. B.; Michl, J. Singlet Fission. *Chem. Rev.* **2010**, *110*, 6891–6936.

(13) Weiss, L. R.; Bayliss, S. L.; Kraffert, F.; Thorley, K. J.; Anthony, J. E.; Bittl, R.; Friend, R. H.; Rao, A.; Greenham, N. C.; Behrends, J. Strongly Exchange-Coupled Triplet Pairs in an Organic Semiconductor. *Nature Phys.* **2017**, *13*, 176–181.

(14) Tayebjee, M. J. Y.; Sanders, S. N.; Kumarasamy, E.; Campos, L. M.; Sfeir, M. Y.; McCamey, D. R. Quintet Multiexciton Dynamics in Singlet Fission. *Nature Phys.* **2017**, *13*, 182–188.

(15) Matsuda, S.; Oyama, S.; Kobori, Y. Electron Spin Polarization Generated by Transport of Singlet and Quintet Multiexcitons to Spin-Correlated Triplet Pairs During Singlet Fission. *Chem. Sci.* **2020**, *11*, 2934–2942.

(16) Hartzler, D. A.; Slipchenko, L. V.; Savikhin, S. Triplet-Triplet Coupling in Chromophore Dimers: Theory and Experiment. *J. Phys. Chem. A* **2018**, *122*, 6713–6723.

(17) Taffet, E. J.; Beljonne, D.; Scholes, G. D. Overlap-Driven Splitting of Triplet Pairs in Singlet Fission. *J. Am. Chem. Soc.* **2020**, *142*, 20040–20047.

(18) Abraham, V.; Mayhall, N. J. Revealing the Contest between Triplet-Triplet Exchange and Triplet-Triplet Energy Transfer Coupling in Correlated Triplet Pair States in Singlet Fission. *J. Phys. Chem. Lett.* **2021**, *12*, 10505–10514.

(19) Johnson, P. A.; Bartolotti, L. J.; Ayers, P. W.; Fievez, T.; Geerlings, P. In *Modern*

Charge Density Analysis; Gatti, C., Macchi, P., Eds.; Springer: New York, 2012; pp 715–764.

(20) Ito, S.; Nagami, T.; Nakano, M. Molecular Design for Efficient Singlet Fission. *J. Photochem. Photobio. C: Photochem. Rev.* **2018**, *34*, 85–120.

(21) Tsuneda, T.; Taketsugu, T. Singlet Fission Initiating Organic Photosensitizations. *Sci. Rep.* **2024**, *14*, 829(1–16).

(22) Tsuneda, T.; Taketsugu, T. Singlet Fission Initiating Triplet Generations of BODIPY Derivatives Through π-Stacking: A Theoretical Study. *Sci. Rep.* **2022**, *12*, 19714–19722.

(23) Tsuneda, T.; Taketsugu, T. Roles of Singlet Fission in the Photosensitization of Silicon Phthalocyanine. *J. Phys. Chem. Lett.* **2023**, *14*, 11587–11596.

(24) Wang, L.; Olivier, Y.; Prezhdo, O. V.; Beljonne, D. Maximizing Singlet Fission by Intermolecular Packing. *J. Phys. Chem. Lett.* **2014**, *5*, 3345–3353.

(25) Tsuneda, T.; Singh, R. K.; Nakata, A. Relationship Between Orbital Energy Gaps and Excitation Energies for Long-Chain Systems. *J. Comput. Chem.* **2016**, *37*, 1451–1462.

(26) Kendall, R. A.; Dunning Jr., T. H.; Harrison, R. J. Electron Affinities of the First-Row Atoms Revisited: Systematic Basis Sets and Wave Functions. *J. Chem. Phys.* **1992**, *96*, 6796–6806.

(27) Krylov, A. I. Size-Consistent Wave Functions for Bond-Breaking: The Equation-of-Motion Spin-Flip Model. *Chem. Phys. Lett.* **2001**, *338*, 375–384.

(28) Shao, Y.; Head-Gordon, M.; Krylov, A. I. The Spin-Flip Approach Within Time-Dependent Density Functional Theory: Theory and Applications to Diradicals. *J. Chem. Phys.* **2003**, *118*, 4807–4818.

(29) Iikura, H.; Tsuneda, T.; Yanai, T.; Hirao, K. A Long-Range Correction Scheme for Generalized-Gradient-Approximation Exchange Functionals. *J. Chem. Phys.* **2001**, *115*, 3540–3544.

(30) Tsuneda, T.; Hirao, K. Long-Range Correction for Density Functional Theory. *WIREs Comput. Mol. Sci.* **2014**, *4*, 375–390.

(31) Becke, A. D. Density-Functional Exchange-Energy Approximation with Correct Asymptotic Behavior. *Phys. Rev. A* **1988**, *38*, 3098–3100.

(32) Lee, C.; Yang, W.; Parr, R. G. Development of the Colle-Salvetti Correlation-Energy Formula into a Functional of the Electron Density. *Phys. Rev. B* **1988**, *37*, 785–789.

(33) Tsuneda, T.; Singh, R. K.; Nakata, A. On Low-Lying Excited States of Extended Nanographenes. *J. Comput. Chem.* **2017**, *38*, 2020–2029.

(34) Postils, V.; Ruiperez, F.; Casanova, D. Mild Open-Shell Character of BODIPY and Its Impact on Singlet and Triplet Excitation Energies. *J. Chem. Theory Comput.* **2021**, *17*, 5825–5838.

(35) Frisch, M. J.; Trucks, G. W.; Schlegel, H. B.; Scuseria, G. E.; Robb, M. A.; Cheeseman, J. R.; Scalmani, G.; Barone, V.; Petersson, G. A.; Nakatsuji, H. et al. Gaussian 16 Revision A.03. 2016; Gaussian Inc. Wallingford CT.

(36) Schmidt, M. W.; Baldridge, K. K.; Boatz, J. A.; Elbert, S. T.; Gordon, M. S.; Jensen, J. H.; Koseki, S.; Matsunaga, N.; Nguyen, K. A.; Su, S. et al. General Atomic and Molecular Electronic Structure System. *J. Comput. Chem.* **1993**, *14*, 1347–1363.

(37) Dean, J. C.; Oblinsky, D. G.; Rafiq, S.; ; Scholes, G. D. Methylene Blue Exciton States Steer Nonradiative Relaxation: Ultrafast Spectroscopy of Methylene Blue Dimer. *J. Phys. Chem. B* **2016**, *120*, 440–454.